JMATPRO	Journal of Advanced Materials and Processing 10 (4): 57-65, Autumn 2022 http://jmatpro.iaun.iau.ir 20.1001.1.2322388.2022.10.4.6.5

Research Paper

A Biosensor for the Detection of Type b3a2 Related to Chronic Myelogenous Leukemia by Using Locked Nucleic Acid, Molecular Switching, Magnetic Nanoparticles, and Enzymatic Signal Amplification

Hamzeh Amoshahi[1], Mohammad Reza Mohammad Shafiee[1*], Shabnam Kermani[2], Mehrosadat Mirmohammadi[3]

1. Department of Chemistry, Najafabad Branch, Islamic Azad University, Najafabad, Iran.
2. Department of Tissue Engineering, Najafabad Branch, Islamic Azad University, Najafabad, Iran.
3. Department of Chemistry, Shahreza Branch, Islamic Azad University, Shahreza, Iran.

ARTICLE INFO

Article history:

Received 14 May 2023
Accepted 11 October 2023
Available online 1 November 2022

Keywords:
Biosensor
Fe3O4 nanoparticles
Nucleic acid
Chronic Myelogenous Leukemia.

ABSTRACT

A novel electrochemical method was developed for the detection of Type b3a2 (BCR/ABL gene) as a biomarker of Chronic Myelogenous Leukemia that is based on the use of locked nucleic acid incorporating LNA switching, Fe_3O_4 nanoparticles (NP_S), and enzymatic signal amplification. The quality of the biosensor was proven by field emission scanning electron microscopy, transmission electron microscopy, X-ray diffraction, and electrochemical impedance spectroscopy tests. The LNA probe was modified by NH_2 and biotin at its 3-end and 5-end, respectively. After unfolding the loop-and-stem structure of the probe, it was hybridized with Type b3a2, which makes the biotin stay away from the surface of Fe_3O_4 NP_S. Type b3a2 can be evaluated quantitatively using electrochemical detection of the benzoquinone enzymatic product with the presence of H_2O_2 and hydroquinone via the particular interaction between SA-HRP and biotin. Particular and selective Type b3a2 detection was obtained over an extensive concentration range from 50 femtometer (fM) to 5 micrometer (µM) in a low limit of detection of 17 fM via the biosensor.

Citation: Amoshahi, H.; Mohammad Shafiee, M.R.; Kermani, SH.; Mirmohammadi, M. (2022). A Biosensor for the Detection of Type b3a2 Related to Chronic Myelogenous Leukemia by Using Locked Nucleic Acid, Molecular Switching, Magnetic Nanoparticles, and Enzymatic Signal Amplification, Journal of Advanced Materials and Processing, 10 (4), 57-65. Dor: 20.1001.1.2322388.2022.10.4.6.5

[*] **Corresponding Author:**
E-Mail: dr.mshafiee98@gmail.com

1. Introduction

A clonal myeloproliferative disease that is caused by the neoplastic transformation of the elementary hemopoietic stem cell is Chronic Myelogenous Leukemia (CML) [1, 2]. Commonly, no observable symptoms are shown in the early stage of CML patients, and the chronic course lasts between 3 to 5 years. The diagnosis of CML becomes difficult due to these phenomena. There have been several studies on how the translocation of chromosome 9 to 22 generated chimeric oncogene BCR/ABL, which can result in CML pathogenesis. BCR/ABL gene can be created in approximately all cases of CML patients [3]. Type b3a2 is one of the several varieties of BCR/ABL genes, which is the most common mutation type and is usually studied in scientific research. Therefore, early monitoring and diagnosis of the disease will be afforded by the BCR/ABL gene determination that leads to the improvement of the detection ability of minimal leukemia cells remaining in the cases, especially behind the bone marrow transplantation. Electrochemical aptamer-based biosensors have recently been expanded because of their rising significance in the sensitive, simple, low-cost, and quick diagnosis of disease [4-7]. In addition, there are expanded applications of Fe_3O_4 in biotechnology, exactly like analytical chemistry [8-10], because of its strong super-paramagnetic property, high adsorption ability, large surface area, excellent biocompatibility, easy preparation, quantum size effect, and low toxicity. Moreover, since probes with hairpin structures have high selectivity due to hybridizing with perfect complementary targets that are able to distinguish the targets with mismatch sequences, they are more attractive probes for deoxyribonucleic acid (DNA) biosensors [11]. Also, LNA can resist degradation with the use of nucleases [12, 13]. These perfect properties let LNA probes ameliorate the hybridization selectivity and sensitivity for nucleic acid-sensing. In this paper, a new electrochemical method for detecting BCR/ABL genes (Type b3a2) according to hairpin LNA probes, Fe_3O_4 nanoparticles modified Glassy carbon electrode (GCE), and enzymatic signal amplification has been offered. A simple electrochemical biosensor was fabricated. In general, the aim of producing the magnetic nano biosensor is to detect CML in the early stages, to reduce the detection time from one month and several weeks to less than one hour, and especially to reduce the detection costs with high sensitivity and accuracy.

2. Experimental

2.1. General

The DNA and LNA subsequence that were consumed in this project were synthesized by Bioneer Company (South Korea) (Table 1). In diethylpyrocarbonate (DEPC) treated Milli-Q water synthetic DNA sequences were liquefied by autoclaved sterilization and were retained frozen. Thionine, dry sodium acetate, ethylene glycol, Pentane-1,5-dial (glutaraldehyde), polyethylene glycol 3350 (PEG-3350), Nafion (ethanesulfonyl fluoride, 2-[1-[difluoro-[(trifluoroethenyl) oxy] methyl]-1,2,2,2-tetrafluoroethoxy] -1,1,2,2, -tetrafluoro-, with tetrafluoroethylene -perfluoro-3,6-dioxa-4-methyl-7-octenesulfonic acid copolymer), alumina (Aluminium oxide), and streptavidin labelled horseradish peroxidase (SA-HRP) were purchased from Sigma corporation. Materials provided by the Merck company were iron (III) chloride hexahydrate ($FeCl_3 \cdot 6H_2O$), Tri(2-carboxyethyl) phosphine hydrochloride (TCEP), 1,6-hexane diamine (Hexamethylenediamine), sodium dodecyl sulphate (SDS), tris(hydroxymethyl-1) amino methane (Tris), disodium ethylene diamine tetra acetic acid (EDTA) and H_2O_2. A 100-fold dilution of SA-HRP was obtained by 10 mM phosphate buffer solution. (PBS, pH 7.0). Reagents all had analytically pure grade, applied with no filtration process. There are some buffer solutions that were applied during this research process described below:

Electrochemistry determination buffer: phosphate buffer solution (0.1 M) (pH 7.0, PBS, 0.1 M), achieved by a mixture of the stock solution of Na_2HPO4 and NaH_2PO_4; DNA hybridization buffer: 1 × SSC (15 mM trisodium citrate with 150 mM NaCl); Probe immobilization buffer: NaCl (1.0 M), TCEP (1.0 M), EDTA (1.0 mM), and Tris-HCl (10 mM) (pH 7.0).

Table 1. Oligonucleotide Sequences Employed in the Present Work

Name	Sequence 5’ to 3’
LNA probe	3′-NH_2-$(CH2)_6$ -GGC CG AGA GTT CAA AAG CCC TTC CG GCC-biotin -5′
Target DNA	GAA GGG CTT TTG AAC TCT
1-base mismatch DNA	GAA GCG CTT TTG AAC TCT
3-base mismatch DNA	GAA GCG CTT ATG TAC TCT
non-complementary DNA	ACG TGG TCC CCA GCT CTC

Using a μAutolab III (Eco Chemie B.V.) potentiostat/ galvanostat and a traditional three-electrode cell, all electrochemical measurements were conducted. A saturated calomel electrode (SCE), an improved glassy carbon electrode, and a platinum wire were used as the reference electrode, working electrode, and auxiliary electrode. JEOL JEM-2100 instrument was utilized for obtaining transmission electron microscopy (TEM) images. A Bruker D4 diffractometer in the 2θ range of 10°-80° at a scanning rate of 1° min^{-1} with graphite-monochromatized Cu Kα radiation (l =1.5406 nm) was applied for x-ray diffraction (XRD) measurement. Field emission scanning electron microscope (FE-SEM) evaluations were performed on a TESCAN MIRA3-XMU FE-SEM. Every one of the evaluations and analyses was performed at ambient temperature.

2.2. Synthesis of the aldehyde-functionalized magnetic nanoparticles (AF-MNPs) precursor

The amino-Fe_3O_4 NPs were synthesized based on the hydrothermal reduction method [14, 15]. In order to do this, 2.0 g of $FeCl_3{\cdot}6H_2O$ (as a single Fe ion source), 4.0 g of anhydrous sodium acetate (CH3COONa), and 13 g of a solution of 1,6-hexane diamine (hexamethylenediamine) were appended to 80 mL ethane-1,2-diol (ethylene glycol). The mentioned solution was stirred under potent stirring for 30 min at 50 °C. After that, the mixture was heated in a Teflon-lined autoclave at 198°C for 6 hours. Then, the degree of the solution was decreased to room temperature. After gathering the Fe_3O_4 nanoparticles (MNPs) and using a magnet, they were cleaned with ethanol and water (3 times) to efficiently pick up the solvent and released 1, 6-hexane diamine (Hexamethylenediamine). Then, 10mg of amino-Fe_3O_4 nanoparticles were added drop by drop into a Pentane-1,5-dial (glutaraldehyde) mixture (20 mL) of 2.5 % (v/v) in 10 mM Phosphate Buffered Solution (PBS) (pH 7), followed by shaking the suspension for two hours at room temperature in a nitrogen atmosphere.

2.3. Fabrication of the biosensor for detecting target DNA

Before surface modification, alumina slurry (0.3 mm and 0.05 mm) was used to polish the Glassy carbon electrode (GCE) frequently to obtain a mirror-like surface. In the following, consecutive sonication in double distilled water and dry ethanol were done for 5 min. After that, drying in the airstream was performed. After that, 6 mL of Nafion (2.5 wt %) was put onto the cleaned electrode. Then, the drying process at room temperature was done; the electrode was plunged into 3 mM Thionine solution (10 min), and, after that, washed with water. Eventually, the electrode was incubated for 8 h with 1 mg. mL^{-1} AF-MNPs in 0.02 M PBS (pH 7.0). This process needs to be shaken repeatedly to refuse the aggregation of the AF-MNPs. In order to refuse cross-contamination, the electrode was cleaned with water to start the fabrication process. Before immobilization, the LNA probe was treated respectively with a 70 oC water bath for 30 minutes and an ice-cold water bath for 10 minutes to prevent the formation of polymer [16]. To LNA immobilization, the AF-MNPs/Thi/Nafion/GCE was plunged in the immobilization buffer solution including 5.0 $\times 10^{-7}$ M LNA (18 h) to achieve a monolayer probe. After that, the electrode (LNA/AF-MNPs/Thi/Nafion/GCE) was washed with 10 mM Tris-HCl (three times) to eradicate the immobilized non-fixing LNA. Immersion of the electrode was performed into the hybridization buffer, including a specific concentration of target DNA for 45 min at ambient temperature in a container that has been humidified for hybridization with LNA. A washing buffer was used for washing the electrode (three times) to eradicate the un-hybridized target DNA after hybridization. The achieved electrode was noted as Target/Probe/AF-MNPs/Thi/Nafion/GCE.

2.4. SA-HRP immobilization

Incubation of the Target/Probe/AF-MNPs/Thi/ Nafion/GCE was done for 60 min in 0.05% PEG-3350 solution (obtained in 0.1 M pH 7.0 PBS) so that non-specific binding is avoided. The amount of 5 mL SA-HRP was dropped into the surface of the electrode. Then, using 0.1 M PBS (pH 7.0), the electrode was washed three times. It was then incubated at ambient temperature for 40 min. After that, PBS (0.01 M) with a pH of 7.0 was used to wash the electrode (three times) and the electrode was dried at ambient temperature. The achieved electrode was recorded as SA-HRP/Target/Probe/AF-MNPs/Thi/Nafion/GCE.

3. Results and discussion

3.1. Characterization of MNPs

TEM, FE-SEM, and XRD were applied to characterize Amino-Fe_3O_4 nanoparticles. Figure. 1A illustrates the FE-SEM image of amino-Fe_3O_4 nanoparticles. According to Figure 1A, the amino-Fe_3O_4 nanoparticles showed a significantly smaller size compared to the naked particles that approve the coating of 1, 6 hexanediamine [17, 18]. Small nanoparticles are created by adding amine, which makes sites with more convenient nucleation compared to the case without amine. Hence, the size of Fe_3O_4 is bigger than that of Fe_3O_4-NH_2. Moreover, the morphology of Fe_3O_4-NH_2 is characterized by TEM (Fig. 1B). The mean particle sizes of Fe_3O_4, that revealed permissible dispersibility were 14.3 nm. The single-nano crystal nature of amino-Fe_3O_4 was verified by the nanometre-scale details of crystal-

lattice fringes in the higher-magnification pictures of the sample. The interplanar spacing of approximately 0.25 nm clearly corresponds with the spacings of the planes of Fe_3O_4. Powder XRD was used to examine the crystallinity and the structure of the amino-MNPs and AF-MNPs. There is an apparent similarity between the standard powder diffraction data from JCPDS No. 19-0629 and the relative intensity of diffraction peaks for Fe_3O_4 and the peak position (Fig. 1C). The XRD patterns of MNPs did not show any considerable variation before and after adding GLU. The diffraction peaks were broadened to separately specify the nanocrystalline nature of the samples. Particularly, Fe_3O_4 had larger crystallinity and particle size due to the powerful intensities and peak widths of its XRD pattern.

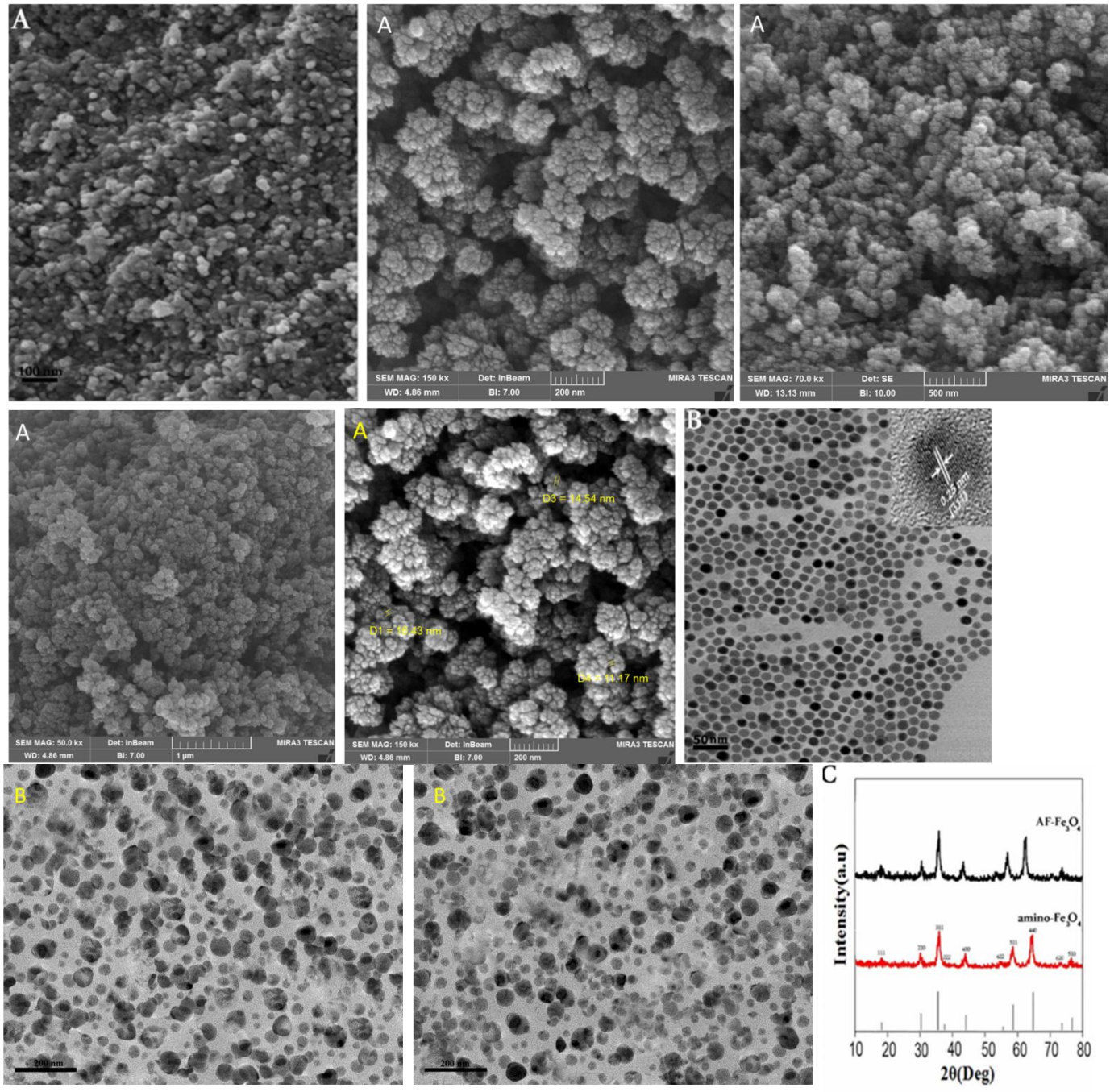

Fig. 1. (A): FE-SEM images of amino-Fe_3O_4 NPs (B): TEM images of Fe_3O_4-NH_2 NPs (C): XRD patterns of AF- Fe_3O_4 NPs and amino- Fe_3O_4 NPs.

3.2. Analysis strategy

The present study employed the LNA probe tagged by the NH group at its 30-end. Scheme 1 shows the electrode preparation process as well as the target DNA detection approach. The collection of the Nafion was first conducted on a bare GCE surface. Then, the tionin was collected on the Nafion/GCE surface. It was followed by collecting the AF-MNPs

on the Thi/Nafion/GCE surface. The reaction between thionine and glutaraldehyde present in AF-MNPs involves an imine reaction, whose mechanism is illustrated in Figure 2. Finally, the LNA with stem-ring structure was mounted on the surface of AF-MNPs/Thi/Nafion/GCE. Prior to hybridization, a hairpin structure is preserved by the immobilized probe. The location of the labeled biotin at the 50-end of the hairpin LNA probe was close to the surface of the electrode. Hence, the biotin lacks the capability of interacting with SA-HRP owing to the steric hindrance impact. Unfolding of the hairpin structure was observed owing to the hybridization with the target DNA. Hence, the labeled biotin was maintained far from the electrode surface. Thus, with particular conjugation with biotin, the SA-HRP was immobilized on the electrode. In order to make benzoquinone the immobilized HRP catalyzed the hydroquinone's chemical oxidation reaction with H_2O_2. Eventually, the hybridization event was monitored using the reduction signal of benzoquinon

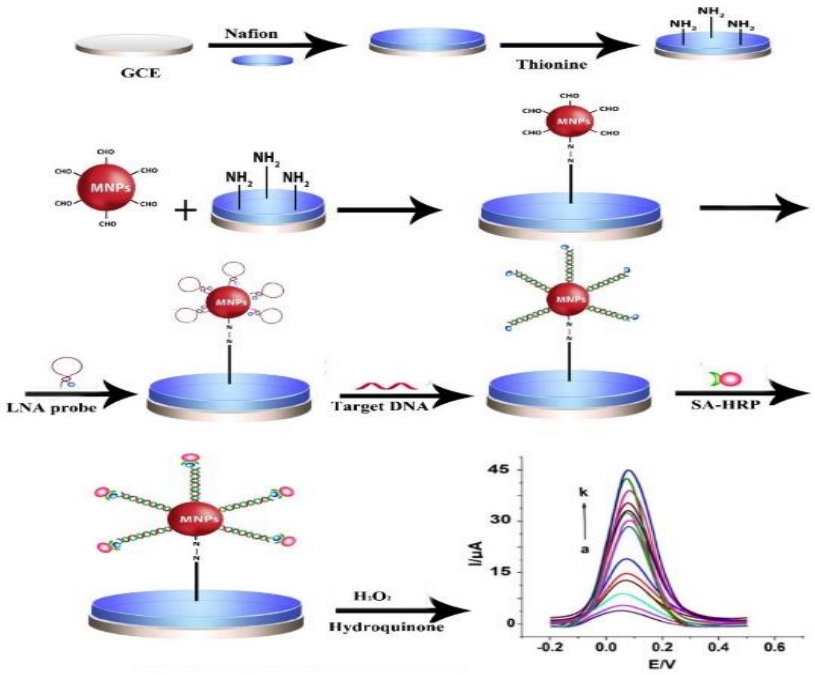

Scheme 1. Schematic of the fabrication route of the biosensor.

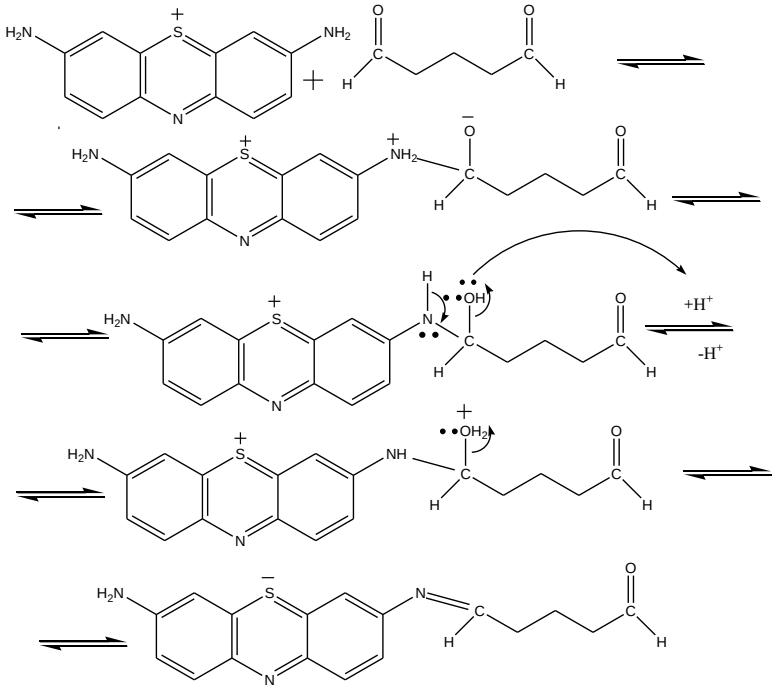

Scheme 2. Schematic of binding mechanism of glutaraldehyde to thionine

3.3. Electrode characterization

As an efficient and acceptable approach to investigate the interface characteristics of surface improved electrodes, EIS can describe accurate data in the improvement process on the impedance variations. The EIS was conducted on various electrodes in Fe $(CN)_6^{3-/4-}$ (5 mM), such as KCl (0.1 M). Based on Figure. 2, the evaluation of the electron transfer resistance (Rct) was performed at bare GCE around 230 Ω (a). It was evident that there is a smaller semicircle matching to a smaller Rct value of 85 Ω, following improvement by Thi/Nafion (b), representing improvement of Thionine (the electro active material) by Nafion through opposite charged absorption on the electrode surface. After the formation of AF-MNPs on the improved electrode, Rct was amplified (1260 Ω, curve c). Therefore, it is worth mentioning that immobilization was performed effectively through the interaction between the amino groups of Thi and AF-MNPs. As a result of hampering the probe accessibility to the electrode surface, an impedance enhancement was observed due to AF-Fe_3O_4 framework. A clear semicircle was evident followed by mounting the hairpin LNA probes on the electrode surface showing an increased electron-transfer resistance (1780 Ω, curve d). The reason for this may be electrostatic repulsion between Fe $(CN)_6^{3-/4-}$ redox probe and negative charges of the LNA phosphate backbone, discovering that LNA probes prosperously immobilized on the electrode surface. Following hybridizing the hairpin LNA probe with the target DNA, was noticed in value of Ret value (2380 Ω, curve e). The negatively charged backbone of DNA resulted in increased repulsive forces to the Fe $(CN)_6^{3-/4-}$probe, leading to this phenomenon. The hybridization between the target DNA and the hairpin LNA probe was approved by the enhanced Ret value. The Ret value experienced a considerable rise to 3430 Ω after SA-HRP was immobilized on the surface of the electrode with the particular interaction between biotin and streptavidin (curve f). Based on these findings, electrode fabrication processes were fruitful.

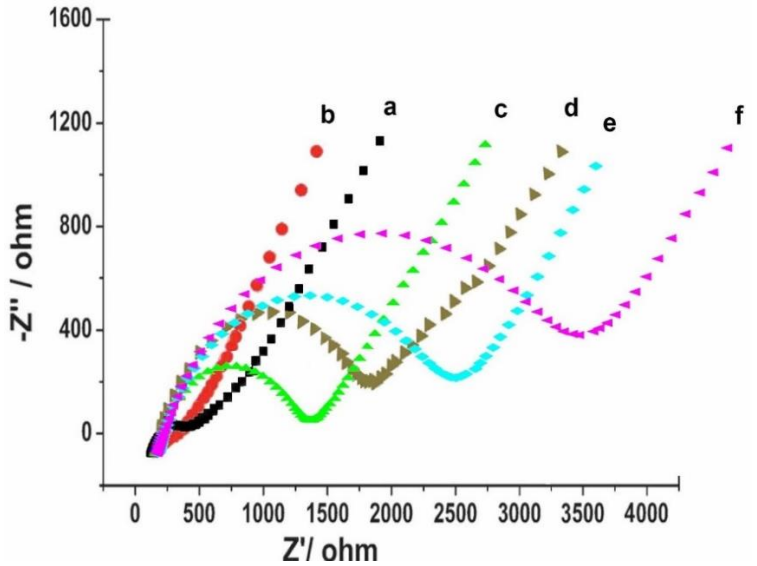

Fig. 2. The electrochemical impedance spectroscopy (EIS) of various electrodes were done in Fe $(CN)_6^{3-/4-}$ (5 mM) including KCl (0.1 M): bare GCE (a), Thi/Nafion/GCE (b), AF-Fe_3O_4/ Thi/Nafion/GCE (c), LNA/AF-Fe_3O_4/ Thi/Nafion/GCE (d), DNA/LNA/AF-Fe_3O_4/Thi/Nafion/ GCE (e), SA-HRP/ DNA/LNA/AF-Fe_3O_4/Thi/Nafion/ GCE (f).

3.4. Optimization of experimental conditions

The determination performance of the fabricated biosensor can be influenced by the determination conditions, including hybridization time and probe immobilization time. To enhance the biosensor's sensitivity and efficiency, using voltammetry, the determination condition was optimized. Figure. 3A shows the probe immobilization time impact on the reduction current of benzoquinone. After 18 h immobilization, the utmost current was achieved. So, this immobilization time was chosen as the optimum condition. Adjusting the hybridization period from 30 to 120 min was the process that checked the influence of hybridization time on the benzoquinone reduction signal (Fig. 3B). The reduction current gradually rose with the time rising from 30 to 45 min, afterward, with further accelerating the hybridization time, the current increased very slightly. So, 45 min was adopted during our trials in order to certify the relatively high determination and hybridization efficiency.

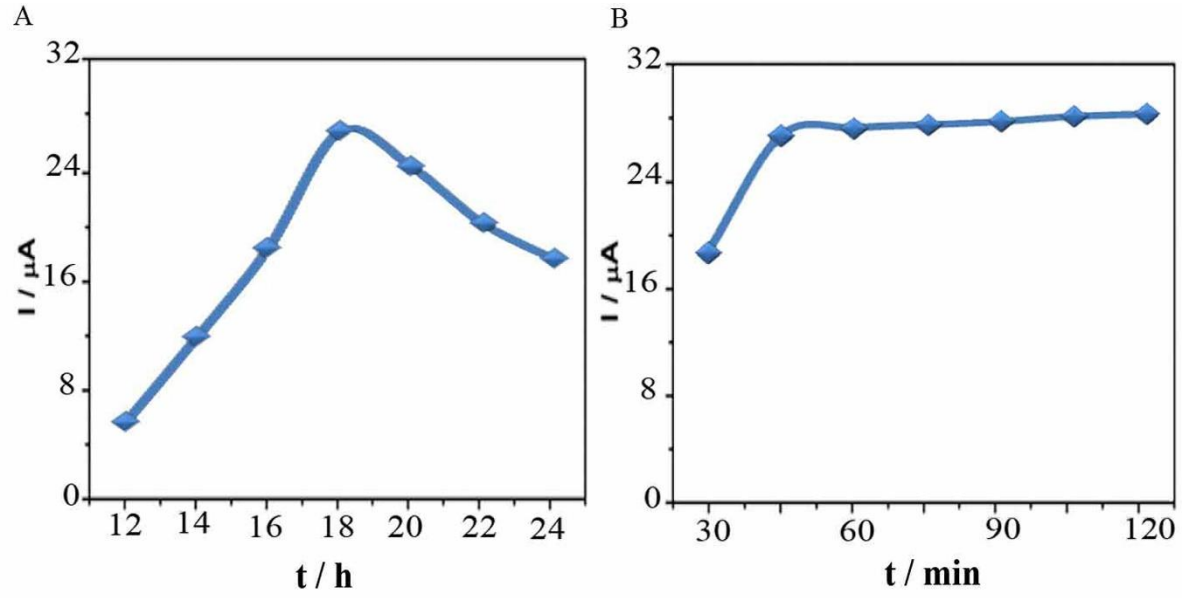

Fig. 3. A. Influence of probe immobilization time on the current intensity, B. Influence of hybridization time on the current intensity.

3.5. Detection sensitivity and selectivity

Fig. 4A indicates the voltametric curves of the developed biosensor after hybridization with various target DNA concentrations. It can be due to the loop-stem structure of the probe being discovered with high concentrations of target DNA, which result in the improved immobilization of HRP on the surface of the electrode. As revealed by the obtained results, the presented approach has the capability of monitoring DNA hybridization. The current intensity was improved by increasing of target DNA concentration. Figure. 4A represents the linear connection between the current variations and the logarithm of target DNA concentration changing from 50 fM to 5 µM was represented in the insert graph. The linear regression equation is expressed as $I = 4.96 \log C + 69.7$ ($R= 0.989$). Connection between the current variations and the logarithm of target DNA concentration changing from 50 fM to 5 µM was represented in the insert graph. The linear regression equation is expressed as $I = 4.96 \log C + 69.7$ ($R= 0.989$). The estimated detection limit was 17 fM ($S/N = 3$). Followed by the probe hybridization with different DNA sequences, a comparison was made between the current responses for checking the detection selectivity. As can be seen in Figure. 4B, the signals of benzoquinone followed by the probe hybridized with target DNA, single base mismatched DNA, three base mismatched DNA, and non-complementary DNA. The maximum current signal was acquired due to the hybridization with the target DNA sequence, representing an efficient target DNA hybridization using the LNA probe. Furthermore, it is possible to paste SA-HRP on the electrode surface owing to the particular interaction between the biotin and SA-HRP at the 50-end of the probe. Moreover, the reduction current of benzoquinone was negligible, followed by the probe hybridization with the non-complementary DNA. In other words, the variant nucleic acids can be persuasively discriminated by the biosensor, demonstrating a super-selective assessment for nucleic acids. In comparison with the hybridization with the complementary DNA, smaller values of the reduction currents were obtained in the case of single base mismatched and three base mismatched sequences; however, they enhanced a bit compared with the non-complementary sequence. Thus, the developed biosensor maintained great selectivity for the detection of hybridization, and this was shown by the proposed assay approach that was capable of efficiently discriminating complementary DNA sequences.

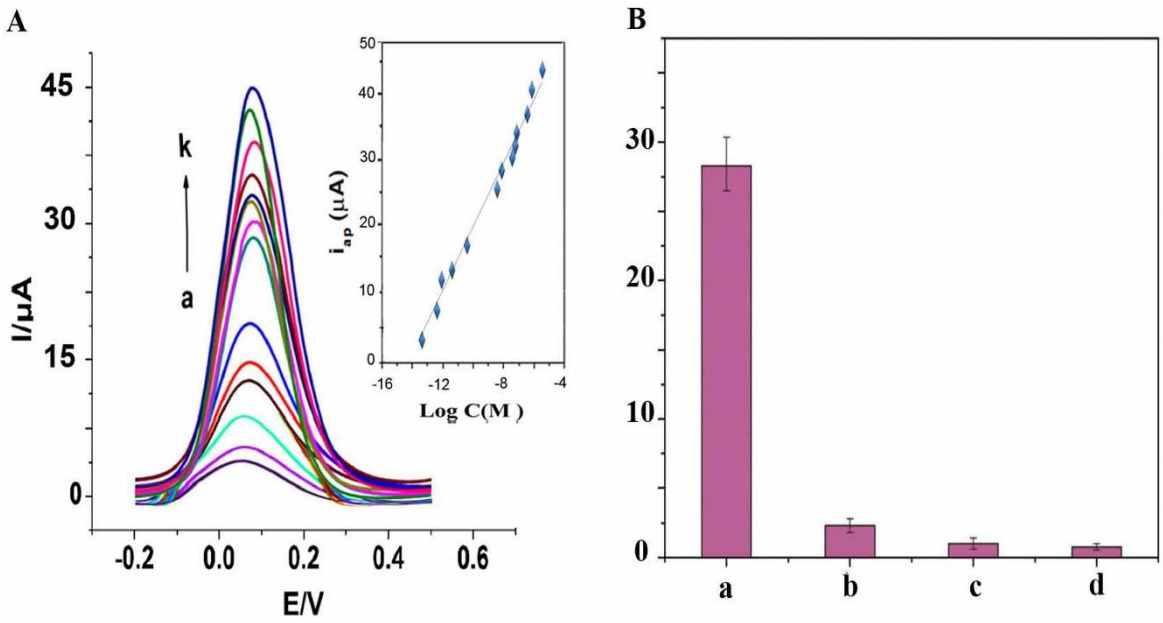

Fig. 4. A: The voltammetric curves the linear relationship diagram between the current changes and the logarithm of target DNA concentration changes from 50 fM to 5 μM, The linear relationship diagram between the current changes and the logarithm of target DNA concentration changes from 50 fM to 5 μM (A, inset), B: Comparison of currents after probe hybridization with target DNA (a), single base mismatched DNA (b), three base mismatched DNA (c), and non-complementary DNA (d), respectively.

3.6. Repeatability and reproducibility of the biosensor

In addition to sensitivity and selectivity, other highly significant properties of biosensors in practical use, including clinical diagnoses are reproducibility and repeatability. The first characteristic of the responses was obtained for 1μM of target DNA with several biosensors. For the detection of Type b3a2, five electrodes were independently produced under similar conditions. The obtained relative standard deviation (RSD) was 6.9%. Moreover, permissible repeatability was achieved for the developed biosensor. The RSD value (n=7) for the current response to Type b3a2 (1 μM) achieved by the biosensors was 4.9%, for target DNA. According to the obtained results, permissible reliability was evident in the presented biosensor preparation protocol. Furthermore, 86% of the initial current response remained by the fabricated biosensor for Type b3a2 followed by its keeping at 4 °C for 25 days. The current responses fell, possibly due to the gradual deactivation of the immobilized biomolecules. Therefore, the biosensor could be highly stable.

4. Conclusions

This paper presents a particular and sensitive hybridization assay for BCR/ABL gene (Type b3a2) based on Fe_3O_4 nanoparticles, hairpin LNA switching, and enzymatic amplification of an electrochemical signal. A considerable rise was observed in the electrochemical active region of the substrate electrode due to a large specific area in Fe_3O_4 nanoparticles, allowing more aldehyde deposition on the surface of the electrode for immobilizing the improved probe. The determination sensitivity was ameliorated because of these factors. This assay is capable of discriminating several nucleic acid sequences according to the special structure of hairpin LNA. The determination approach was used for the selective and sensitive determination of 17 fM expression levels. In the early diagnosis of cancers, the detection of sensitive cancer biomarkers is essential. Thus, this method plays a unique role in clinical diagnosis.

Acknowledgment

The authors thank from Department of Chemistry, Najafabad Branch, Islamic Azad University, Najafabad, Iran for financial supports of this work.

Conflicts of interest

The authors declared no conflicts of interest in this work.

Authors' Contribution

M.R. Mohammad Shafiee contributed to supervision, visualization, conceptualization, validation, formal analysis, investigation, and writing the original draft of the manuscript; H. Amoshahi contributed to writing the manuscript and investigation; S. Kermani and M. Mirmohammadi contributed to the project administration, writing, and editing the manuscript. The final version of the manuscript was approved by all authors.

References

[1] P.J. Fialkow, S.M. Gartler, A. Yoshida, "Clonal origin of chronic myelocytic leukemia in man", Proc. Natl. Acad. Sci. U.S.A.,Vol. 58, 1967,pp. 1468-1471.
[2] H.M. Kantarjian, A. Deisseroth, R. Kurzrock, "Chronic myelogenous leukemia: A Concise Update", Blood.Vol. 82, 1993, pp. 691-703.
[3] E.C. Jorge, T. Moshe, K. Hagop, "Chronic myelogenous leukemia: A review", Am. J. Med., Vol. 100, 1996, pp. 555-570.
[4] J. Wang, "From DNA biosensors to gene chips", Nucleic Acids Res., Vol. 28, 2000, pp. 3011-3016.
[5] D. Zhang, Y. Chen, H.Y. Chen, X.H. Xia, "Silica-nanoparticle-based interface for the enhanced immobilization and sequence-specific detection of DNA", Anal. Bioanal. Chem., Vol. 379, 2004, pp. 1025-1030.
[6] K.J. Feng, Y.H. Yang, Z.J. Wang, J.H. Jiang, G.L. Shen, R.Q. Yu, "A nano-porous CeO2/Chitosan composite film as the immobilization matrix for colorectal cancer DNA sequence-selective electrochemical biosensor", Talanta., Vol. 70, 2006, pp. 561-565.
[7] C.D. Riccardi, K. Dahmouche, C.V. Santilli, P.I. Costa, H, Yamanaka, "Immobiliza-tion of streptavidin in sol-gel films: application on the diagnosis of Hepatitis C virus", Talanta., Vol. 70, 2006, pp. 637-643.
[8] S. Laurent, D. Forge, M. Port, A. Roch, C. Robic, L.V. Elst, "Magnetic iron oxide nanoparticles: synthesis, stabilization, vectorization, physicochemical characterizations, and biological applications", Chem. Rev., Vol. 108, 2008, pp. 2064-2110.
[9] J. Yang, E.K. Lim, H.J. Lee, J. Park, S.C. Lee, K. Lee, " Fluorescent magnetic nanohybrids as multimodal imaging agents for human epithelial cancer detection", Biomaterials., Vol. 29, 2008, pp. 2548-2555.
[10] A. Kaushik, P.R. Solanki, A.A. Ansari, B.D. Malhotra, S. Ahmad, "Iron oxide-chitosan hybrid nanobiocomposite based nucleic acid sensor for pyrethroid detection", Biochem. Engin. J., Vol. 46, 2009, pp. 132-140.
[11] C.J. Yang, L. Wang, Y. Wu, Y. Kim, C.D. Medley, H. Lin, W. Tan, "Synthesis and investigation of deoxyribonucleic acid/locked nucleic acid chimeric molecular beacons", Nucleic Acids Res., Vol. 35, 2007, pp. 4030-4041.
[12] K. Martinez, M.C. Estevez, Y. Wu, J.A. Phillips, C.D. Medley, W. Tan, "Locked nucleic acid based beacons for surface interaction studies and biosensor development", Anal. Chem., Vol. 81, 2009, pp. 3448-3454.
[13] S. Laschi, I. Palchetti, G. Marrazza, M. Mascini, "Enzyme-amplified electrochemical hybridization assay based on PNA, LNA and DNA probe-modified micro-magnetic beads", Bioelectrochem., Vol. 76, 2009, pp. 214-220.
[14] L. Wang, J. Bao, L. Wang, F. Zhang, Y. Li, "One-pot synthesis and bioapplication of amine-functionalized magnetite nanoparticles and hollow nanospheres", Chem. Eur. J.,Vol. 12, 2006, pp. 6341.
[15] A. Norouzian Baghani, A.H. Mahvi, M. Gholami, N. Rastkari, M. Delikhoon, "One-Pot synthesis, characterization and adsorption studies of amine-functionalized magnetite nanoparticles for removal of Cr (VI) and Ni (II) ions from aqueous solution: kinetic, isotherm and thermodynamic studies", J. Environ. Health Sci. Eng., Vol. 14, 2016, pp. 11.
[16] X. Mao, J. Jiang, X. Xu, X. Chu, Y. Luo, G. Shen, R. Yu, "Enzymatic amplification detection of DNA based on "molecular beacon" biosensors", Biosens. Bioelectron.,Vol. 23, 2008), pp. 1555.
[17] Y. Tan, M. Chen, Y. Hao, "High efficient removal of Pb (II) by amino-functionalized Fe_3O_4 magnetic nano-particles", Chem. Eng. J., Vol. 191, 2012, pp. 104-111.
[18] G.Y. Li, Y.R. Jiang, K.L. Huang, P. Ding, J. Chen, "Preparation and properties of magnetic Fe_3O_4-chitosan nanoparticles", J. Alloys Compd., Vol. 466, 2008, pp. 451-456.